Temporal profile of the LCLS photocathode ultraviolet drive laser tolerated by the microbunching instability[*]

Juhao Wu,[†] P. Emma, Z. Huang, and C. Limborg

Stanford Linear Accelerator Center, Stanford University, Stanford, CA 94309

M. Borland

Advanced Photon Source, Argonne National Laboratory, Argonne, IL 60439

The high quality LCLS electron beam generated in the photoinjector is subject to many instabilities in the downstream acceleration and compression. The instability can be initiated by any density modulation of the electron beam generated at the photocathode. In this paper, we prescribe the tolerance on the initial electron beam density modulation possibly introduced by the ultraviolet (uv) laser at the cathode. Our study shows that with a matched Landau damping laser-heater, the initial rms density modulation of the electron beam at the photocathode must be less than 5% to ensure the FEL lasing and saturation.

Submitted to the 22nd International Linear Accelerator Conference (LINAC 2004)

I. INTRODUCTION

The success of the free-electron laser (FEL) calls for a high quality electron beam characterized by high peak current, small slice emittance, and small slice energy spread. However, such a high quality electron beam generated from a photocathode gun is subject to various impedance sources along the downstream acceleration and compression. This can lead to beam quality degradation and beam instability. Specifically, the impedance (associated with space charge, wakefield, and coherent synchrotron radiation) and momentum compaction factor in the linac and compressors act as an amplifier for initial density and energy modulations. Since the slice emittance and slice energy spread are extremely small, Landau damping is not effective in suppressing all these potential instabilities. Such instabilities can increase the slice energy spread and emittance, and therefore degrade FEL lasing. FEL operation calls for best achievable beam quality; yet, unnecessarily high quality renders it more susceptible to instabilities associated with beamline impedance and momentum compression. To address this quandary, a laser-heater [1] is introduced into the Linac Coherent Light Source (LCLS) beamline. The laser-heater is composed of a short undulator with resonant laser-electron energy modulation in a weak magnetic chicane (see [1]). It is designed to be an adjustable control, which will impose a limited increase on the slice energy spread to the level where FEL lasing is still guaranteed. This 'procured' increase is designed to enhance

Landau damping such that downstream instabilities can be suppressed.

Density and energy modulations could be initiated by shot noise in the electron beam born at the photocathode. Such shot noise is normally small. But temporal modulation on the ultraviolet (uv) laser pulse itself can be transferred to the electron beam at birth. As discussed above, any initial electron beam density or energy modulations can be amplified. If this happens, the FEL lasing may be affected. Hence, we need to specify the tolerance of any density modulations of the electron beam generated from the photocathode of the gun.

The approach we take is to first set the requirements on the electron beam quality which we need at the entrance of the undulator. We then ask what tolerance on the density modulation of the electron beam is needed at the initial photocathode to make sure that the requirement we look for at the entrance of the undulator can be satisfied.

II. SYSTEM PARAMETERS WITH LASER-HEATER

In our study, we take the nominal LCLS accelerator system setup with the laser-heater included. The LCLS FEL parameters are listed in Table I. A schematic of the LCLS layout is shown in Fig. 1 indicating the location of laser-heater. The laser-heater is to be installed upstream DL1 (the first dog-leg transport line in Fig. 1) where the electron beam energy is at $E = 135$ MeV. Parameters for the laser-heater are listed in Table II. In our study, we used a total temporal compression factor of 30. Hence, if we require the rms slice relative energy spread to be about 1×10^{-4} when the beam energy reaches $E = 14.1$ GeV at the entrance of the undulator, then the laser-

---

TABLE I: Main parameters for the LCLS FEL.

Parameter	Symbol	Value
electron energy	γmc^2	14.1 GeV
bunch charge	Q	1 nC
bunch current	I_f	3.4 kA
transverse norm. emittance	$\varepsilon_{x,y}^n$	1 μm
average beta function	$\beta_{x,y}$	25 m
undulator period	λ_u	0.03 m
undulator field	B	1.3 T
undulator parameter	K	3.64
undulator length	L_u	130 m
FEL wavelength	λ_r	1.5 Å
FEL parameter	ρ	4.8×10^{-4}

TABLE II: Main parameters for the LCLS laser-heater.

Parameter	Symbol	Value
electron energy	$\gamma_0 mc^2$	135 MeV
average beta function	$\beta_{x,y}$	10 m
transverse rms beam size	$\sigma_{x,y}$	190 μm
undulator period	λ_u	0.05 m
undulator field	B	0.33 T
undulator parameter	K	1.56
undulator length	L_u	0.5 m
laser wavelength	λ_L	800 nm
laser rms spot size	σ_r	175 μm
laser peak power	P_L	1.2 MW
Rayleigh range	Z_R	0.6 m
maximum energy modulation	$\Delta\gamma_L(0)mc^2$	80 keV
rms local energy spread	$\sigma_{\gamma_L}mc^2$	40 keV

heater should give a maximum rms slice energy spread of $\sigma_E = 47$ keV, assuming that the longitudinal phase space area is conserved. We note that there are multiple sources of dilution to the longitudinal phase space area. This amount of slice energy spread then determines the Landau damping strength to suppress instabilities in the accelerator system. Therefore, this with laser-heater in place imposes a limit on the maximum amount of density modulations in the electron beam born at the laser cathode of the injector.

The laser-heater introduces energy modulation at the laser wavelength of 800 nm. A schematic of the laser-heater is shown in Fig. 2. On the other hand, the chicane provides $R_{52} \approx \eta_x \approx 20$ mm, which will induce a path length difference of $\sigma_{\Delta z} = R_{52}\sqrt{\langle x'^2 \rangle}$. Given that $\sqrt{\langle x'^2 \rangle} \sim 20$ μrad, we have $\sigma_{\Delta z} \sim 400$ nm $\gg \bar{\lambda}_L \equiv \lambda_L/(2\pi) \approx 127$ nm. Hence, the energy modulation induced by the laser-heater will be immediately washed out by the second half of the chicane, and will not introduce density modulation at $\lambda_L = 800$ nm. Therefore, due to this longitudinal position smearing, the induced energy modulation becomes purely slice energy spread; and, the laser-heater induced energy modulation will not be converted into any density modulation.

III. SIMULATION DETAILS

If the electron beam at birth has density or energy modulations, then due to the longitudinal space charge effect, there will be space charge oscillation. Such an oscillation will convert density modulation into energy modulation and vice versa. This oscillation essentially stops when the electron beam energy reaches certain value, which is a function of the density modulation wavelength. For example, assuming an electron beam of rms transverse size of 200 μm, and peak current of 100 Amp,

for the microbunching wavelength $\lambda \in [50, 300]$ μm, the space charge oscillation period is about 1.5 to 3.5 m, if the electron beam energy is around 10 MeV. So, for typical device of length of a few meters in the beam line, there would be space charge oscillation [1]. The space-charge oscillation period is a sensitive function of beam energy. For the same parameter set, the oscillation period is 10 to 45 m for a 30 MeV energy beam. Therefore space charge oscillation for a given distance can be insignificant at high beam energy.

In our study, we take the following two approaches. In the first approach, we introduce a density modulation at the end of injector, where the electron beam energy reaches 135 MeV. As what we explained above, at this energy, and for the modulation wavelength we are interested in, there is no longer a significant space charge oscillation. In the second approach, we introduce a density modulation in the electron beam when it was born at the cathode. This simulates a realistic situation where the electron beam density modulation is due to temporal modulation of the laser. Details of these two approaches are described below.

Approach I: we take a PARMELA output distribution at the end of injector section at 135 MeV with 200,000 macroparticles, where there is no density modulation or energy modulation in the beam distribution function. We then superimpose density modulation at specific modulation wavelength and amplitude. In doing so, the longitudinal momentum correlation is preserved. We also preserve the correlation of the local slice energy spread. We also preserve the transverse emittance of the beam and its correlations. Under these conditions, we then increase the total number of particles to 2 million to reduce numerical shot noise. In addition, we use Halton sequence
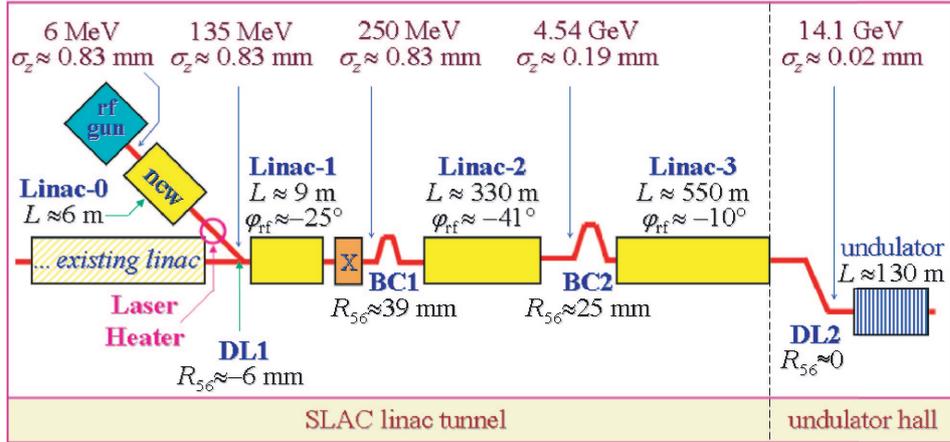
FIG. 1: (Color) Layout of the LCLS accelerator system with Landau damping laser heater at 135 MeV.
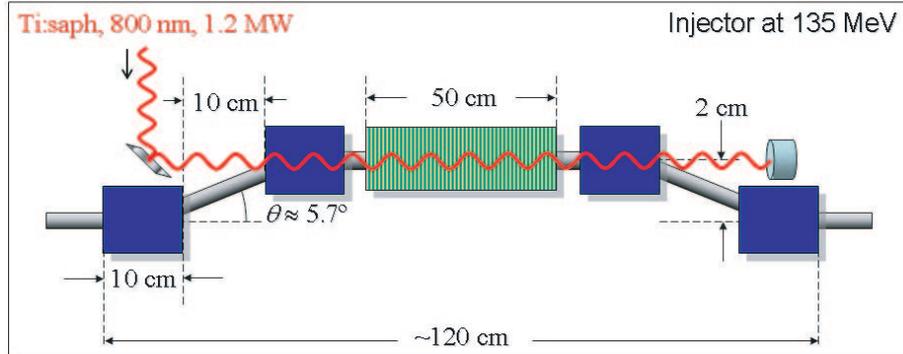

FIG. 2: (Color) Layout of the LCLS laser heater inside a magnetic chicane at 135 MeV.

TABLE III: Summary of the parameters and results for the microbunching and final slice relative energy spread.

		Set I							Set II		
Energy modulation amplitude at cathode	keV	0							0		
Density modulation amplitude at cathode	%	0							8		
Energy modulation amplitude at injector end	keV	0							0.3	3.1	1.2
Density modulation amplitude at injector end	%	1						4	0.7	1.0	1.3
Density modulation wavelength	μm	15	30	60	100	150	200	150	50	150	300
Final slice rms relative energy spread at 14 GeV	10^{-4}	0.9	0.9	0.9	0.8	0.9	0.8	1.0	1.1	1.0	1.0

"quiet-start" to generate these 2 million particles in all the 6-D distributions.

Approach II: in this approach, the microbunching density modulation is superimposed at the cathode emitting surface. The macroparticle number is reduced to be 1 million, since fully ASTRA space charge simulation in the injector is very time consuming. Macroparticles are tracked through the photoinjector via ASTRA simulation code. This beam distribution function at the end of injector is then used as input to transport through the rest of accelerator system using the Elegant simulation code. In contrast to the electron beam used in approach I, there exists energy modulation in the beam at 135 MeV.

Even with use of the Halton sequence, numerical noise remains an issue in the full simulation. This is because when we compute energy kick in the simulation, we use electron beam current spectrum times the impedance. In order to further reduce the noise effect, a high pass filter is introduced in the Elegant simulation [1] to cut the impedance above a certain frequency, so that the high frequency numerical noise will not be amplified. In our study, we simulate a single frequency modulation. When the gain is high enough, the instability can also become nonlinear. Once the system runs into the nonlinear regime, harmonics of the original modulation frequency will show up. Hence in order to account for nonlinear behaviors, we set the high pass filter slightly higher than the second harmonic of the original frequency. In doing so, modulation with frequencies higher than the second harmonic is filtered out, however, modulations with frequencies between the second harmonic (including the second harmonic) and the original frequency are preserved in our simulation.

IV. SIMULATION RESULTS

For approach I, we prepare an initial $\pm 1\%$ density modulation with 6 different wavelengths at the injector end. We also did one simulation with an initial $\pm 4\%$ density modulation to check linearity of the instability gain. In all these simulations, the laser-heater introduces about a 40 keV slice rms energy spread. The results are summarized in Table III. The slice rms relative energy spread is the average of the central 20 μm portion of the entire beam. Each slice is 0.5 μm long, to match the slippage distance of the FEL in the undulator.

For approach II, we prepared an initial $\pm 8\%$ density modulation with 3 different wavelength at the cathode. In these simulations, the laser-heater introduces the maximum allowable slice rms energy spread of 47 keV. The results are summarized in Table III. The slice rms relative energy spread is defined according to approach I.

To illustrate how the beam instability will degrade the longitudinal phase space, and also to demonstrate how effectively the laser-heater could Landau damp the instability, here we show a typical phase space comparison between a matched laser-heater and no laser-heater.
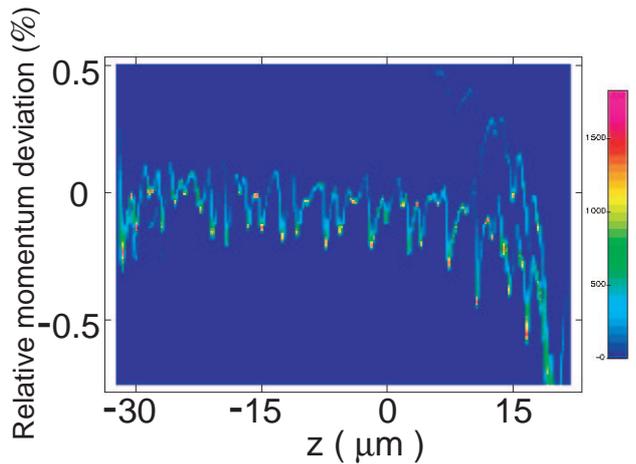

FIG. 3: (Color) Longitudinal phase space at the entrance of undulator. This is for the case of an initial $\pm 8\%$ density modulation at 150 μm in set II simulation without laser-heater.
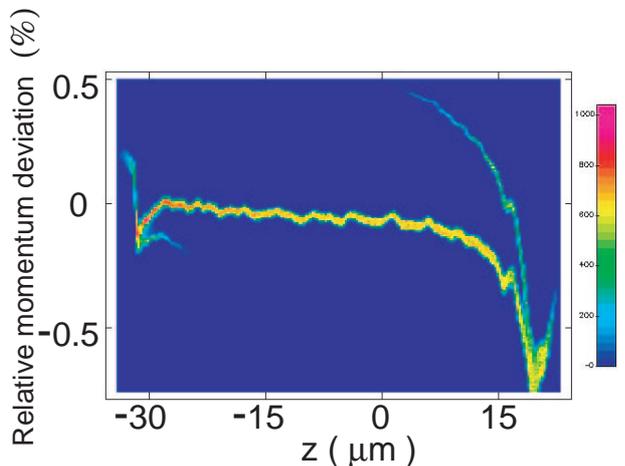

FIG. 4: (Color) Longitudinal phase space at the entrance of undulator. This is for the case of an initial $\pm 8\%$ density modulation at 150 μm in set II simulation with a matched laser-heater.

(A matched laser-heater is a device where the transverse laser beam size is approximately equal to that of the electron beam.) Figure 3 shows the longitudinal phase space at the entrance of the undulator when no laser-heater is used, and Fig. 4 shows the corresponding case with a matched laser-heater. These figures are an example from the approach II simulation, and the initial $\pm 8\%$ density modulation is at wavelength of $\lambda = 150$ μm. In Fig. 3, we find a very large final energy modulation. The period is about 150 μm/30 = 5 μm, which indicates that the ini-
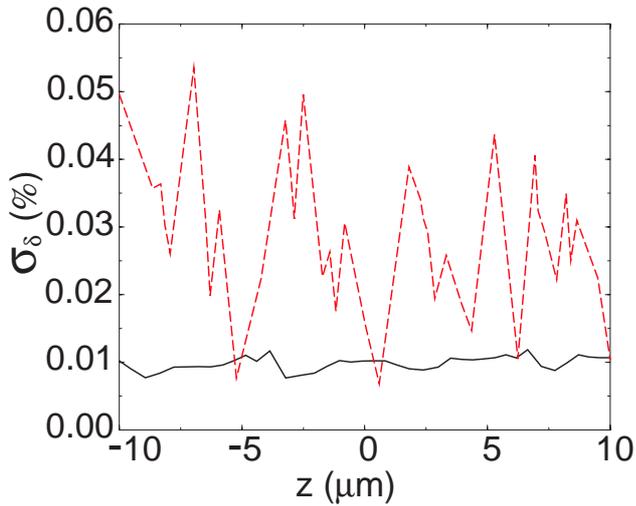
FIG. 5: (Color) Slice rms relative energy spread at the entrance of undulator. This is for the case of an initial $\pm$ 8% density modulation at 150 μm in set I simulation. Solid curve stands for the result with a matched laser-heater; and dashed curve for the result without laser-heater.

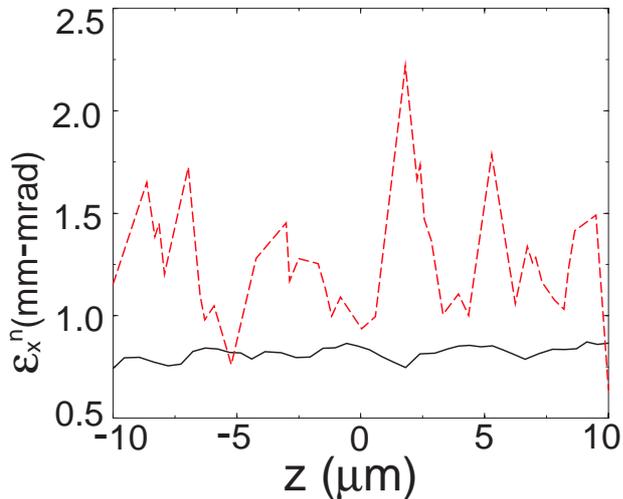FIG. 6: (Color) Slice normalized x emittance ϵ_x^n at the entrance of undulator. This is for the case of an initial $\pm$ 8% density modulation at 150 μm in set I simulation. Solid curve stands for the result with a matched laser-heater; and dashed curve for the result without laser-heater.

tial 150 μm density modulation leads to a large energy modulation after the 30 times compression. Besides this initial 150 μm modulation, the second harmonic is also clearly shown. This indicates that the system has evolved into the nonlinear regime. This proves that we should set the high pass filter above the second harmonic to allow it to grow. With a matched laser-heater, the results differ significantly as illustrated in Fig. 4. The effectiveness of the matched laser-heater is seen in the greatly reduced amplitude of energy modulation at the 5 μm period. The quantity which will affect the FEL lasing is the slice en-

ergy spread within the slippage length. In the LCLS case, the slippage length is about 0.5 μm. We then plot, in Fig. 5, the slice rms relative energy spread along the electron beam. The matched laser-heater clearly limits the final slice rms relative energy spread to $\sigma_\delta < 1.0 \times 10^{-4}$ at the central portion of the electron beam. In contrast, the final slice rms relative energy spread without laser-heater is much too high to permit FEL operation. Similar conclusions can be drawn for the slice normalized x emittance ϵ_x^n. Figure 6 shows that the slice normalized x emittance, ϵ_x^n along this central portion of the electron beam is limited to value less than 1 mm-mrad when the matched laser-heater is used. Without laser-heater, the ϵ_x^n is much larger and prohibits FEL operation.

For the other wavelength, the conclusion are the same. To make sure that the final slice energy spread meets the FEL requirements, a matched laser-heater is critically effective in suppressing the instabilities and therefore necessary.
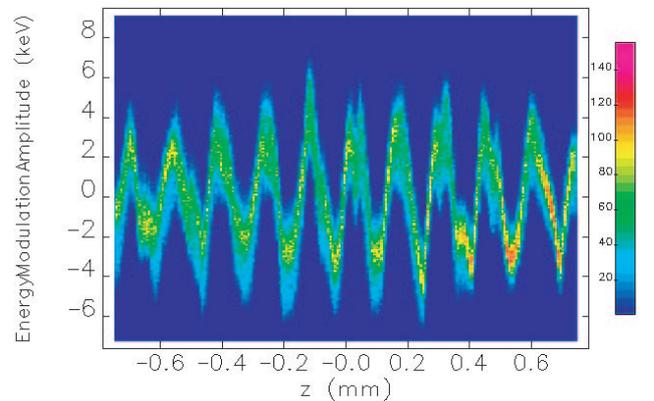

FIG. 7: (Color) Energy modulation along the bunch at the end of photoinjector, but prior to the laser-heater. This is for the case of an initial $\pm$ 8% density modulation at 150 μm in set II simulation.

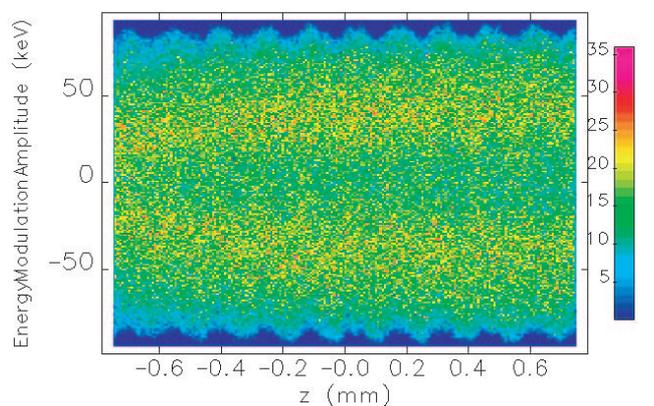

FIG. 8: (Color) Energy modulation along the bunch at the end of a matched laser-heater. This is for the case of an initial $\pm$ 8% density modulation at 150 μm in set II simulation.

V. DISCUSSION

It is important to clarify the distinction between approach I and II.

Table III shows that the initial $\pm 8\%$ density modulation is reduced after the injector. However the known space-charge oscillation results in an accumulated energy modulation in the injector. This residual energy modulation can in turn be reconverted back into a density modulation without the laser-heater. A matched laser-heater induces a slice rms energy spread on the order of 40 keV, which enhances Landau damping and the residual energy modulation is smeared out.

To demonstrate this, in Figs. 7 and 8, we chose the 150 μm wavelength example in approach II. It can be seen in Table III that the density modulation is reduced to the $\pm 1\%$ level and the accumulated energy modulation has increased from zero to ± 3 keV. Relative to the 3 keV slice rms energy spread, this is a 100% modulation as seen in Fig. 7. By contrast, Fig. 8 shows that with a matched laser-heater this accumulated energy modulation is only about 7% of the slice rms energy spread. Landau damping suppresses the reconversion of this residual energy modulation back to a density modulation in BC1. This largely suppresses the downstream instability.

VI. CONCLUSION

In our study, all the simulations are done for density modulation at a specified frequency. The results show that without the laser-heater, the gain of the microbunching is too high to make FEL lasing possible. Shown in Figs. 5 and 6, without the laser-heater, the final slice rms relative energy spread at the entrance of the undulator would be much larger than the 1×10^{-4}, FEL requirement; also, without the laser-heater, the slice normalized x emittance ϵ_x^n would be much larger than the 1 mm-mrad, FEL requirement. Use of a matched laser-heater indicates that the FEL requirement of 10^{-4} for the slice rms relative energy spread and 1 mm-mrad for the slice normalized x emittance can be met with a peak-to-peak electron density modulation as much as $\pm 8\%$ at the photocathode. This we interpret as the maximum density modulation tolerance at birth. Assuming the $\pm 8\%$ modulation for all wavelengths and a relative insensitivity to wavelength in 50 μm to 300 μm interval, we determine this maximum tolerance to be a 5% rms value. Because the electron density modulation is driven by the uv laser pulse. This is therefore the upper limit to the rms noise on the temporal profile of the us laser pulse.

[1] Z. Huang *et al.*, SLAC Report No. SLAC-PUB-10334, 2004.